Construction and Building Materials 60 (2014) 98–110

Contents lists available at ScienceDirect

Construction and Building Materials

journal homepage: www.elsevier.com/locate/conbuildmat

A study of multiple effects of nano-silica and hybrid fibres on the properties of Ultra-High Performance Fibre Reinforced Concrete (UHPFRC) incorporating waste bottom ash (WBA)

R. Yu *, P. Tang, P. Spiesz, H.J.H. Brouwers

Department of the Built Environment, Eindhoven University of Technology, P.O. Box 513, 5600 MB Eindhoven, The Netherlands

HIGHLIGHTS

- Waste bottom ash (WBA) is applied in UHPFRC.
- Modified Andreasen and Andersen particle packing model is used to design UHPFRC.
- Multiple effects of nano-silica and hybrid fibres on the properties of UHPFRC are analyzed.
- Cement hydration process of UHPFRC with and without WBA is investigated.
- Effect of the WBA on the microstructure development of UHPFRC is presented.

ARTICLE INFO

Article history:
Received 11 November 2013
Received in revised form 13 January 2014
Accepted 17 February 2014

Keywords:
Ultra-High Performance Fibre Reinforced Concrete (UHPFRC)
Waste bottom ash (WBA)
Nano-silica
Hybrid fibres
Multiple effects

ABSTRACT

This article addresses the multiple effects of nano-silica and hybrid fibres on the properties of an Ultra-High Performance Fibre Reinforced Concrete (UHPFRC) incorporating waste bottom ash (WBA). The design of the concrete mixtures was based on the aim to achieve a densely compacted matrix, employing the modified Andreasen and Andersen particle packing model. The workability, porosity, flexural and compressive strengths of the UHPFRC are measured and analyzed. The results show that due to the existence of the metallic aluminium particles in WBA, the generated hydrogen can cause some visible macro-cracks in the concrete, which could reduce the mechanical properties of the concrete. However, with a simultaneous utilization of nano-silica and hybrid fibres (steel and polypropylene fibres), the negative influence from the WBA can be effectively minimized and the flexural strength of the UHPFRC can be improved.

1. Introduction

Ultra-High Performance Fibre Reinforced Concrete (UHPFRC) is a combination of high performance concrete matrix and fibres reinforcement. In particular, it is a super plasticized concrete, reinforced with fibres, with improved homogeneity [1]. However, as sustainable development is currently a pressing global issue and various industries have strived to achieve energy savings, the high material cost, high energy consumption and CO_2 emission for UHPFRC are the typical disadvantages that restrict its wider application [2,3]. Hence, in recent years, there have been many attempts to alleviate both the environmental and economic impact of UHPFRC.

As commonly known, the sector of building materials is the third-largest CO_2 emitting industrial sector world-wide, as well as in the European Union [4]. The cement production is said to represent 7% of the total anthropogenic CO_2 emissions [4–6]. Hence, one of the key sustainability challenges for the next decades is to design and produce a type of concrete with less clinker and inducing lower CO_2 emissions than traditional ones, while providing the same reliability, and a better durability [3,7]. Considering the successful achievement on application of UHPFRC for rehabilitation of bridges since 1999 [8], the UHPFRC seems to be one of the candidates to reduce the global warming impact of construction materials. Compared to traditional concrete structures, the ones made with UHPFRC can be much more slender. Hence, due to the fact that the volume of needed concrete can be significantly reduced, the cement amount used for the whole structure can also be reduced so the overall CO_2 footprint of the structure can be lower. Moreover, to reduce the cement amount used for the production of

* Corresponding author. Tel.: +31 (0) 40 247 5469; fax: +31 (0) 40 243 8595.
E-mail address: r.yu@tue.nl (R. Yu).

http://dx.doi.org/10.1016/j.conbuildmat.2014.02.059
0950-0618/

Nomenclature

D_{max}	maximum particle size (μm)	P_{tar}	target curve (–)
D_{min}	minimum particle size (μm)	$\varphi_{v,water}$	water-permeable porosity (%)
q	distribution modulus (–)	m_s	mass of water saturated sample in air (g)
RSS	sum of the squares of the residuals (–)	m_w	mass of water-saturated sample in water (g)
P_{mix}	composed mix (–)	m_d	mass of oven-dry sample (g)

UHPFRC, the optimum packing of the granular ingredients of concrete is considered and applied [9–12]. According to the previous experiences and investigations of the authors [13], by applying the modified Andreasen and Andersen particle packing model it is possible to produce a dense and homogeneous skeleton of UHPFRC with a relatively low binder amount (about 650 kg/m^3). Furthermore, industrial by-products such as ground granulated blast-furnace slag (GGBS), fly ash (FA) and silica fume (SF) have been used as partial cement replacements in UHPFRC [14–16]. Additionally, considering the tremendous consumption of natural resources and serious environmental impact of waste materials, some recycled or waste materials have recently been utilized in the production of UHPFRC [17–20]. Hence, to minimize the disadvantages of UHPFRC, optimized concrete design and reasonable utilization of waste/recycled materials should be the effective methods.

Waste bottom ash (WBA) is one of the by-products of municipal solid waste incineration (MSWI), which can be described as heterogeneous particles consisting of glass, magnetic and paramagnetic metals, minerals, synthetic and natural ceramics, and unburned matter [21]. According to the European Landfill Directive [22], the weathered WBA is considered suitable for land filling or reuse. However, considering the high amount of MSWI residue produced all over the world, European governments encourage the reuse of WBA as a secondary building material ingredient both to prevent the use of non-renewable natural gravels and to avoid excessive land filling. The most widespread practice is the reuse of WBA as an aggregate substitute for road base [23,24], which is subject to strict requirements that are defined by each European country, for example, the Spanish specifications for road construction [25]. Another important way of application of WBA is as an aggregate for concrete [26–28]. Nevertheless, due to the fact that there is metallic aluminium in the WBA, which can react in alkaline solution and produce hydrogen [29–31], many cracks can be generated in the concrete and its mechanical properties could be reduced. To solve this problem, one of the potential methods is the inclusion of fibres, which may effectively restrict the growth of cracks and improve the properties of concrete.

Based on the available literature, the fibres can effectively bridge the cracks generated in concrete [32,33]. Especially the hybrid fibres system, in which short fibres can bridge the microcracks while the long fibres are more efficient in preventing the development of macro-cracks [32,33]. Additionally, in the UHPFRC system, the active pozzolanic materials are commonly utilized, which can effectively improve the interface transition zone between the concrete matrix and fibres and enhance the properties of concrete [34–36]. Hence, it may be a good option to apply the WBA in UHPFRC and produce a greener UHPFRC.

Taking into account the previously mentioned advantages and disadvantages related to the use of WBA in concrete, the aim of this research is to assess the viability of the application of WBA in UHPFRC. The design of the concrete mixtures is based on the aim to achieve a densely compacted cementitious matrix, employing the modified Andreasen and Andersen particle packing model. The nano-silica (nS), steel fibre (SF) and polypropylene fibre (PPF) are included in the concrete design, and their multiple effects on the properties (especially the mechanical characteristics) of the UHPFRC with WBA are investigated. Techniques, like SEM and isothermal calorimetry, are further employed to evaluate the micro- morphology of WBA and the hydration process of binders with WBA.

2. Materials and methods

2.1. Materials

The cement used in this study is Ordinary Portland Cement (OPC) CEM I 52.5 R, provided by ENCI (the Netherlands). A polycarboxylic ether based superplasticizer is used to adjust the workability of concrete. The limestone is used as a filler to replace cement. One commercially available nano-silica in a slurry (AkzoNobel, Sweden) is selected as the pozzolanic material. Two types of sand are used, one is normal sand with the fractions of 0–2 mm and the other one is a microsand with the fraction 0–1 mm (Graniet-Import Benelux, the Netherlands). The waste bottom ash (WBA) used in this study is obtained from a local municipal solid waste incineration (MSWI) plant. The particle size distributions of the used granular materials are shown in Fig. 1. It can be noticed that the particle size distributions of the normal sand and the WBA are similar to each other. Hence, in this study, the WBA is utilized to replace the normal sand. Additionally, two types of fibres are utilized, as shown in Fig. 2: one is straight steel fibre and the other one is a short polypropylene fibre. Additional information on the used materials is shown in Table 1.

To better understand the basic properties of the used WBA, several techniques are employed in this study, and the results are shown in the following part. Fig. 3 presents the morphologies of the normal sand and WBA. As can be seen, the appearance of the WBA and normal sand is relatively similar to each other. Nevertheless, the microscopic analysis shows that, compared to the normal sand, the surface of the WBA is much rougher and contains many fine pores. In addition, some waste threadlike stuff can be often observed at the WBA particles surface, which may act as fibres when applied in concrete and improve its flexural strength. The X-ray fluorescence (XRF) test results of the WBA are shown in Table 2. Note the SiO_2 (55.98%) is the main component in WBA, which is followed by CaO (14.06%) and Fe_2O_3 (11.64%). Moreover, following the method presented in [31], the metallic aluminium content in WBA is around 0.43% by the mass of the WBA. The X-ray diffraction (XRD) pattern of the WBA is illustrated in Fig. 4. The main peaks are marked according to the crystalline diffractogram specification, which are SiO_2, $CaCO_3$, $CaSO_4$ and Fe_2O_3.

Consequently, differently from the normal sand (SiO_2 > 95%), the utilized WBA contains many impurities, which may affect the hydration of cement and microstructure development when applied in concrete.

2.2. Experimental methodology

2.2.1. Mix design of UHPFRC with WBA

For the design of mortars and concretes, several mix design methods can be used. Based on the properties of multimodal, discretely sized particles, De Larrard and Sedran [10,11] postulated different approaches to design concrete: the Linear Packing Density Model (LPDM), Solid Suspension Model (SSM) and Compressive Packing Model (CPM). However, all these design methods are based on the packing fraction of individual components (cement, sand etc.) and their combinations, and therefore it is complicated to include very fine particles in these mix design tools, as it is difficult to determine the packing fraction of such very fine materials or their combinations. Another possibility for mix design is offered by an integral particle size distribution approach of continuously graded mixes, in which the very fine particles can be integrated with relatively lower effort, as detailed in the following. First attempts describing an aimed composition of concrete mixtures, which generally consists of continuously graded ingredients, can be traced already back to 100 years ago. The fundamental work of Fuller and Thompson [37] showed that the packing of concrete aggregates is affecting the properties of the produced concrete. They concluded that a geometric continuous grading of the aggregates in the composed concrete mixture can help to improve the concrete properties. Based on

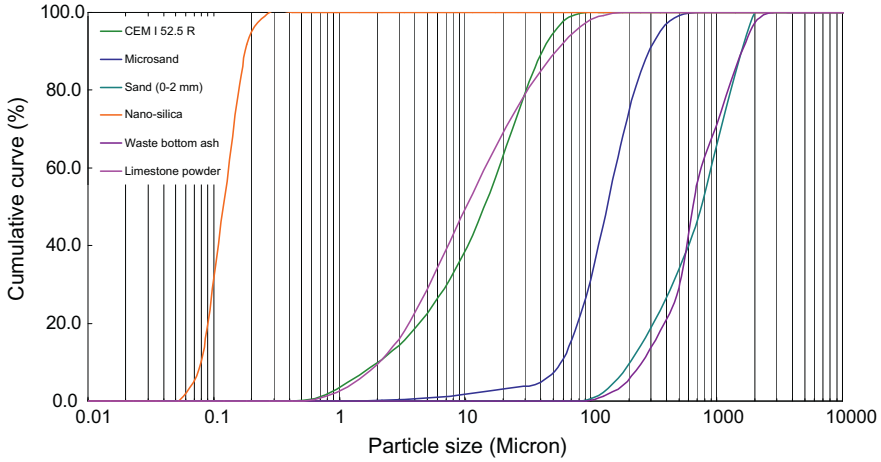

Fig. 1. Particle size distributions of the used materials.

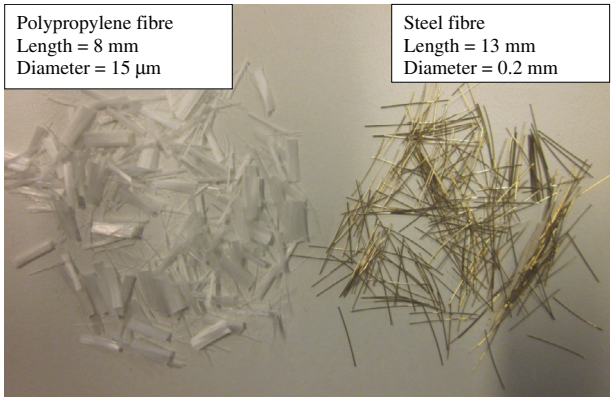

Fig. 2. Steel and polypropylene fibres used in this study.

Table 1
Information of materials used.

Materials	Type	Specific density (kg/m^3)
Cement	CEM I 52.5 R	3150
Filler	Limestone powder	2710
Fine sand	Microsand	2720
Coarse sand	Sand 0–2	2640
Superplasticizer	Polycarboxylate ether	1050
Pozzolanic material	Nano-silica (nS)	2200
Waste materials	Waste bottom ash (WBA)	2690
Fibre-1	Steel fibre (SF)	7800
Fibre-2	Polypropylene fibre (PPF)	920

the investigation of Fuller and Thompson [37] and Andreasen and Andersen [38], a minimal porosity could be theoretically achieved by an optimal particle size distribution (PSD) of all the applied particle materials in the mix, as shown in Eq. (1):

$$P(D) = \left(\frac{D}{D_{max}}\right)^q \quad (1)$$

where D is the particle size (μm), $P(D)$ is a fraction of the total solids being smaller than size D, D_{max} is the maximum particle size (μm), and q is the distribution modulus.

However, in Eq. (1), the minimum particle size is not incorporated, while in reality there must be a finite lower size limit, with which the packing model can be improved. Hence, Funk and Dinger [39] proposed a modified model based on the Andreasen and Andersen Equation. In this study, all the concrete mixtures are designed based on this so-called modified Andreasen and Andersen model, which is shown as follows:

$$P(D) = \frac{D^q - D^q_{min}}{D^q_{max} - D^q_{min}} \quad (2)$$

where D_{min} is the minimum particle size (μm).

The modified Andreasen and Andersen packing model has already been successfully employed for the design of normal density concrete [40–42] and lightweight concrete [43,44]. Different types of concrete can be designed using Eq. (2) by applying different values of the distribution modulus q, as it determines the proportion between the fine and coarse particles in the mixture. Normally, higher values of the distribution modulus ($q > 0.5$) lead to coarse mixture, while lower values ($q < 0.25$) result in concrete mixes which are rich in fine particles [45]. Brouwers et al. [40,46] demonstrated that theoretically a q value range of 0–0.28 would result in an optimal packing. Hunger [42] recommended using a q in the range of 0.22–0.25 in the design of self-compacting concrete (SCC). Hence, here, the modified Andreasen and Andersen packing model is used to design UHPFRC with WBA. Considering that a large amount of fine particles is utilized to produce the UHPFRC, the value of q is fixed at 0.23 in this study, following the recommendations given in [42].

In this research, the modified Andreasen and Andersen model (Eq. (2)) acts as a target function for the optimization of the composition of mixture of granular materials. The proportions of each individual material in the mix are adjusted until an optimum fit between the composed mix and the target curve is reached, using an optimization algorithm based on the Least Squares Method (LSM), as presented in Eq. (3). When the deviation between the target curve and the composed mix, expressed by the sum of the squares of the residuals (RSS) at defined particle sizes, is minimized, the composition of the concrete is treated as the optimal [41].

$$RSS = \sum_{i=1}^{n} \left(P_{mix}(D_i^{i+1}) - P_{tar}(D_i^{i+1})\right)^2 \quad (3)$$

where $P_{mix}(D_i^{i+1})$ is the composed mix, and the $P_{tar}(D_i^{i+1})$ is the target grading calculated from Eq. (2).

Based on the optimized particle packing model, the developed UHPFRC mixtures are listed in Table 3. In total, 30 batches of UHPFRC are designed in this study. Due to the fact that after around 30% normal aggregates (0–2 mm) are replaced by WBA, the workability of the designed concrete is very poor, the WBA is utilized to replace about 20% of the normal aggregate in this study. Moreover, the nano-silica is added in the amount of 0–4% of the total binder amount. One example of the resulting integral grading curve of the composed mixes is shown in Fig. 5. Additionally, according to the literature [2,9,15,16,32,33], the content of steel fibre in fibre reinforced concrete often amounts to around 2% (by volume of the concrete), and the polymer fibre content is less than 0.5% (by volume of the concrete). Hence, in this study, the steel and polypropylene fibres amount is 2% and 0.1–0.4% by the volume of concrete, respectively. Therefore, by analyzing the properties of the different UHPFRCs, it will be possible to evaluate the multiple effects of nano-silica and hybrid fibres on the properties of UHPFRC with WBA.

2.2.2. Selection of the employed mix procedures

The detailed information on the adopted procedures for the production of UHPFRC with WBA is shown in Fig. 6. Due to the inclusion of the WBA and the low water/binder ratio, the mixing time for the designed UHPFRC is relatively long, which is about 10 min. Moreover, mixing is always executed under laboratory conditions with dried and tempered aggregates and powder materials. The room temperature while mixing and testing is constant at around 21 °C.

2.2.3. Workability of UHPFRC

To evaluate the workability of the designed UHPFRC with WBA, the suspension is filled in a conical mold in the form of a frustum (as described in EN 1015-3 [47]) after appropriate mixing following the defined procedure. During the test, the cone

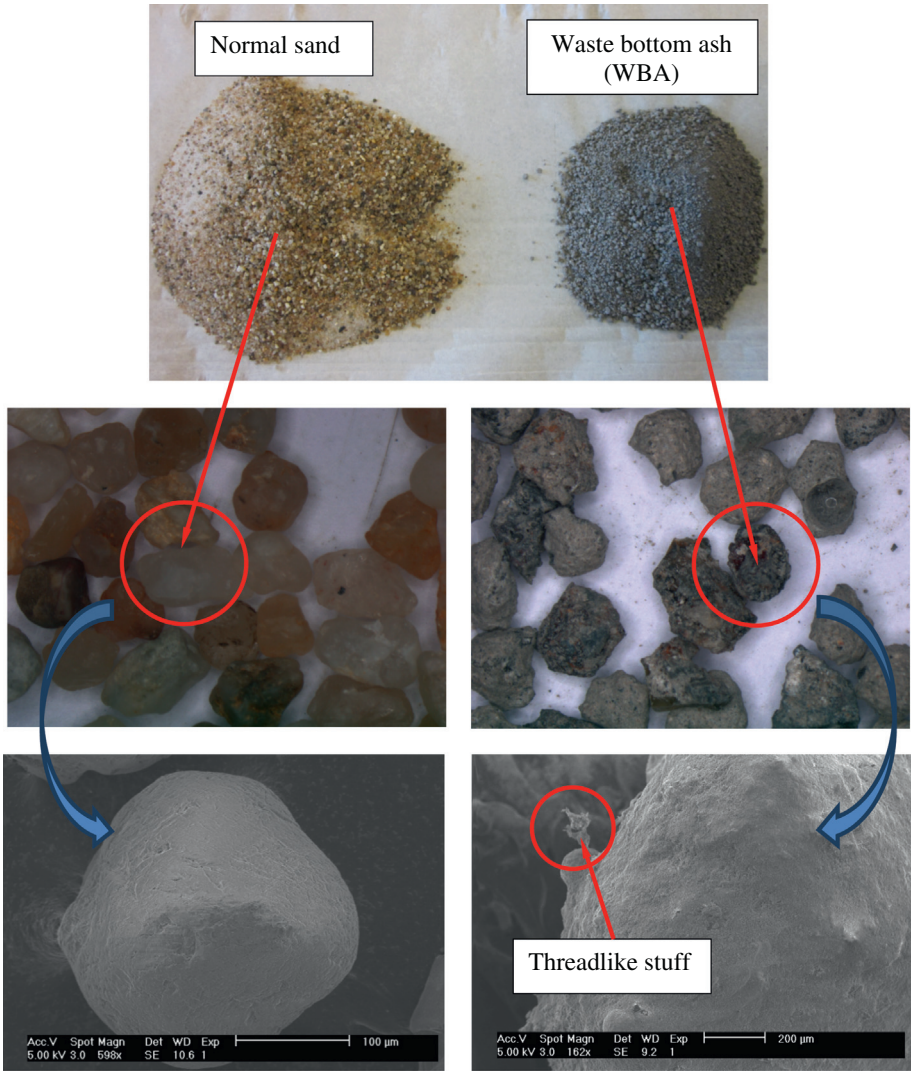

Fig. 3. Morphology comparison of normal sand and waste bottom ash (WBA).

Table 2
Chemical composition of the waste bottom ash (%).

SiO_2	CaO	Al_2O_3[a]	Fe_2O_3	K_2O	Na_2O	MgO	CuO	ZnO	SO_3	P_2O_5	PbO
55.98	14.06	7.70	11.64	0.88	1.86	1.07	0.40	0.55	0.74	0.74	0.31

[a] Metallic aluminium amount: 0.43%.

is lifted straight upwards in order to allow free flow for the mixture without any jolting. In the test, two diameters of the flowed concrete perpendicular to each other are determined. Their mean value represents the slump flow value of the designed UHPFRC.

2.2.4. Porosity of UHPFRC

The porosity of the designed UHPFRC is measured applying the vacuum-saturation technique, which is referred to as the most efficient saturation method [48]. The saturation is carried out on at least 3 samples (100 mm × 100 mm × 20 mm) for each mix, following the description given in NT Build 492 [49] and ASTM C1202 [50].

The water permeable porosity is calculated from the following equation:

$$\varphi_{v,water} = \frac{m_s - m_d}{m_s - m_w} \cdot 100 \quad (4)$$

where $\varphi_{v,water}$ is the water permeable porosity (%), m_s is the mass of the saturated sample in surface-dry condition measured in air (g), m_w is the mass of water-saturated sample in water (g) and m_d is the mass of oven dried sample (g).

2.2.5. Mechanical properties of UHPFRC

After preforming the workability test, the UHPFRC is cast in moulds with the size of 40 mm × 40 mm × 160 mm and compacted on a vibrating table. The prisms are demolded approximately 24 h after casting and subsequently cured in water at about 21 °C. After curing for 28 days, the samples are tested under three-point loading using displacement control and using a testing machine controlled by an external displacement transducer, such that the mid-span deflection rate of the prism specimen is held constant throughout the test. The specimen mid-span deflection rate is 0.10 mm/min, with a span of 100 mm. Afterwards, the compressive strength of the UHPFRC samples is tested according to [51]. During the testing, at least three samples are tested for each batch.

2.2.6. Isothermal calorimetry analysis

To clarify the effect of WBA and nano-silica on the hydration of cement, the heat flow calorimetry test is employed in this study. The recipes of the test samples are shown in Table 5. Before the testing, the samples are mixed for two minutes and then transferred into a sealed glass ampoule, which is then placed into the

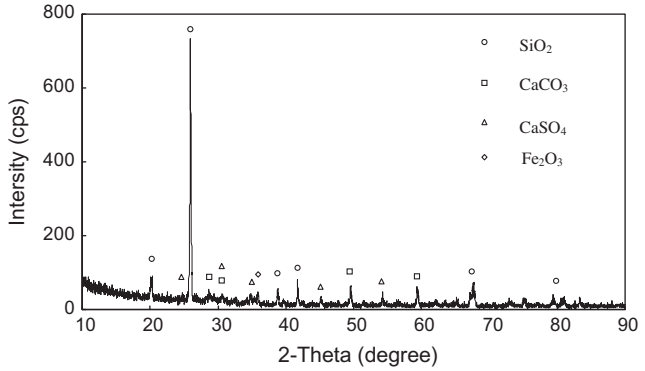

Fig. 4. XRD analysis of the waste bottom ash (WBA).

isothermal calorimeter (TAM Air, Thermometric). The instrument is set to a temperature of 20 °C. After 7 days, the measurement is stopped and the obtained data is analyzed. All results are ensured by double measurements (two-fold samples).

2.2.7. Microscopy analysis

In this study, two microscopes are utilized: one is an optical microscope (maximum magnification of 80×), while the other one is a scanning electron microscope (SEM). The optical microscopy is used to analyze the effect of hybrid fibres on the cracks developments. After curing, the UHPFRC specimens are cut into small fragments with the dimensions of 40 mm × 40 mm × 15 mm. The details of the sampling procedure are illustrated in Fig. 7. Subsequently, the samples are stored in a sealed container before the imaging. The SEM is employed to study the morphology difference between the normal sand and the used WBA.

3. Experimental results and discussion

3.1. Flowability of the designed UHPFRC

From the preliminary experiments it has been found that the addition of WBA can decrease the workability of concrete. After about 20% sand is replaced by WBA, the flowability of the designed concrete drops from 34.5 cm to around 30.0 cm. This phenomenon should be attributed to that the rough and porous surface of the WBA (as shown in Fig. 3) can absorb plenty of water. Furthermore, the effect of nano-silica and hybrid fibres addition on the slump flow ability of fresh UHPFRC mixes incorporating WBA is depicted in Fig. 8. The data illustrates the relationship between the nano-silica and hybrid fibres content and the flowability of the fresh UHPFRC. It is important to notice that with the addition of polypropylene fibres, the flowability of all the UHPFRC mixtures linearly decreases. As shown in Fig. 8, the coefficients of determination (R^2) of all the regression lines are all close to 1, which represent a well linear tendency between the polypropylene fibres amount and the workability of the designed UHPFRC. Moreover, the addition of nano-silica or steel fibres also reduces the workability of the UHPFRC. For instance, in the reference sample (without nano-silica and fibres), the slump flow value is about 30 cm, which drops to around 26.8 and 23.5 cm when nano-silica (2%) or steel fibre (2 vol.%) are added, respectively. Eventually, the slump flow further reduces to about 22.3 cm when the nano-silica (2%) and steel fibre (2 vol.%) are simultaneously added into the UHPFRC. Additionally, when nano-silica (2%), steel fibre (2 vol.%) and polypropylene fibre (0.4 vol.%) are added into the UHPFRC together, the slump flow is the lowest, being about 14.8 cm.

As commonly known, the effect of fibres on the workability of concrete is mainly due to following reasons [32,33]: (1) shape of the fibres is more elongated compared to aggregates, so the surface area at the same volume is higher; (2) stiff fibres change the structure of the granular skeleton, while flexible fibres fill the space between aggregates, which both can increase the porosity of concrete; (3) surface characteristics of fibres differ from that of cement and aggregates, e.g. plastic fibres might be hydrophilic or hydrophobic. In this study, short steel fibres and polypropylene fibres are used, which can produce higher cohesive forces between the

Table 3
Recipes of developed UHPFRC with waste bottom ash (WBA).

No.	C (kg/m^3)	LP (kg/m^3)	M-S (kg/m^3)	N-S (kg/m^3)	WBA (kg/m^3)	nS (kg/m^3)	W (kg/m^3)	SP (kg/m^3)	SF (vol.%)	PPF (vol.%)
1	612.4	262.5	218.7	843.8	210.9	0	201.2	45.9	0	0
2	612.4	262.5	218.7	843.8	210.9	0	201.2	45.9	0	0.1
3	612.4	262.5	218.7	843.8	210.9	0	201.2	45.9	0	0.2
4	612.4	262.5	218.7	843.8	210.9	0	201.2	45.9	0	0.3
5	612.4	262.5	218.7	843.8	210.9	0	201.2	45.9	0	0.4
6	600.2	262.5	218.7	843.8	210.9	12.2	201.2	45.9	0	0
7	600.2	262.5	218.7	843.8	210.9	12.2	201.2	45.9	0	0.1
8	600.2	262.5	218.7	843.8	210.9	12.2	201.2	45.9	0	0.2
9	600.2	262.5	218.7	843.8	210.9	12.2	201.2	45.9	0	0.3
10	600.2	262.5	218.7	843.8	210.9	12.2	201.2	45.9	0	0.4
11	588.0	262.5	218.7	843.8	210.9	24.4	201.2	45.9	0	0
12	588.0	262.5	218.7	843.8	210.9	24.4	201.2	45.9	0	0.1
13	588.0	262.5	218.7	843.8	210.9	24.4	201.2	45.9	0	0.2
14	588.0	262.5	218.7	843.8	210.9	24.4	201.2	45.9	0	0.3
15	588.0	262.5	218.7	843.8	210.9	24.4	201.2	45.9	0	0.4
16	612.4	262.5	218.7	843.8	210.9	0	201.2	45.9	2	0
17	612.4	262.5	218.7	843.8	210.9	0	201.2	45.9	2	0.1
18	612.4	262.5	218.7	843.8	210.9	0	201.2	45.9	2	0.2
19	612.4	262.5	218.7	843.8	210.9	0	201.2	45.9	2	0.3
20	612.4	262.5	218.7	843.8	210.9	0	201.2	45.9	2	0.4
21	600.2	262.5	218.7	843.8	210.9	12.2	201.2	45.9	2	0
22	600.2	262.5	218.7	843.8	210.9	12.2	201.2	45.9	2	0.1
23	600.2	262.5	218.7	843.8	210.9	12.2	201.2	45.9	2	0.2
24	600.2	262.5	218.7	843.8	210.9	12.2	201.2	45.9	2	0.3
25	600.2	262.5	218.7	843.8	210.9	12.2	201.2	45.9	2	0.4
26	588.0	262.5	218.7	843.8	210.9	24.4	201.2	45.9	2	0
27	588.0	262.5	218.7	843.8	210.9	24.4	201.2	45.9	2	0.1
28	588.0	262.5	218.7	843.8	210.9	24.4	201.2	45.9	2	0.2
29	588.0	262.5	218.7	843.8	210.9	24.4	201.2	45.9	2	0.3
30	588.0	262.5	218.7	843.8	210.9	24.4	201.2	45.9	2	0.4
Ref	588.0	262.5	218.7	1054.7	0	0	201.2	45.9	0	0

C: Cement, LP: Limestone powder, M-S: Microsand, N-S: Normal sand, WBA: Waste bottom ash, nS: Nano-silica, W: Water, SP: Superplasticizer, SF: steel fibre, PPF: polypropylene fibre, Ref: reference sample.

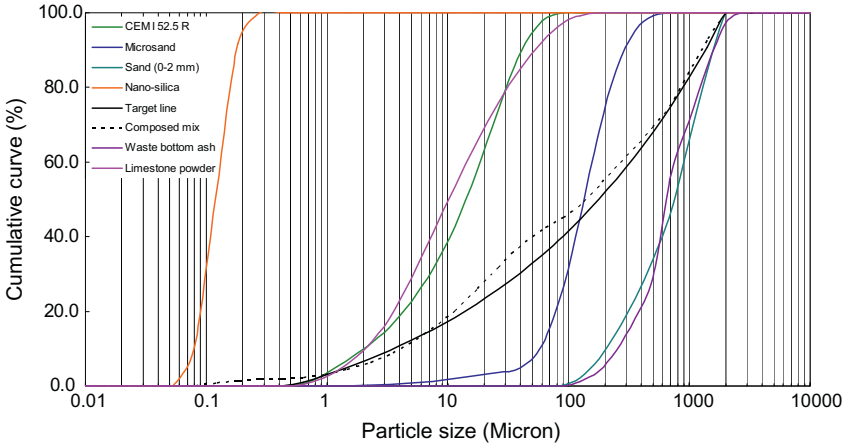

Fig. 5. PSDs of the granular ingredients, the target curve and the resulting integral grading curve of the mix (mix-6 shown as an example).

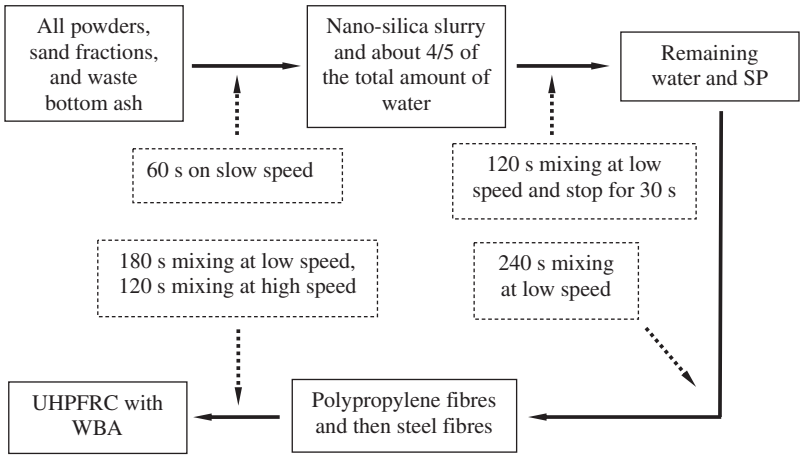

Fig. 6. Detailed information of the mixing procedure adopted for the production of UHPFRC.

Table 4
Effect of the nano-silica, steel fibre and polypropylene fibre on the mechanical properties of the concrete with WBA.

	WBA (%, Mass)	nS (%, Mass)	SF (vol.%)	PPF (vol.%)	C-S (MPa)	F-S (MPa)
Ref.	0	0	0	0	75.8	10.8
1	20	0	0	0	63.3	11.6
2	20	4	0	0	69.6	14.3
3	20	0	2	0	102.9	18.8
4	20	0	0	0.4	62.9	13.5
5	20	4	2	0	113.9	27.9
6	20	4	0	0.4	67.8	17.6
7	20	0	2	0.4	101.9	24.9
8	20	4	2	0.4	112.4	31.7

WBA: Waste bottom ash, nS: Nano-silica, SF: steel fibre, PPF: polypropylene fibre, C-S: Compressive strength (28 days), F-S: flexural strength (28 days), Ref.: reference sample, Mass: Mass fraction of the replaced amount of aggregate or binder in concrete, Vol.: Volume fraction in the total concrete.

Table 5
Recipes of the specimen for the isothermal calorimetry analysis.

No.	C (kg/m^3)	LP (kg/m^3)	M-S (kg/m^3)	N-S (kg/m^3)	WBA (kg/m^3)	nS (kg/m^3)	W (kg/m^3)	SP (kg/m^3)
1	612.4	262.5	218.7	1054.7	0	0	201.2	45.9
2	612.4	262.5	218.7	843.8	210.9	0	201.2	45.9
3	600.2	262.5	218.7	843.8	210.9	12.2	201.2	45.9
4	588.0	262.5	218.7	843.8	210.9	24.4	201.2	45.9

C: Cement, LP: Limestone powder, M-S: Microsand, N-S: Normal sand, WBA: Waste bottom ash, nS: Nano-silica, W: Water, SP: Superplasticizer.

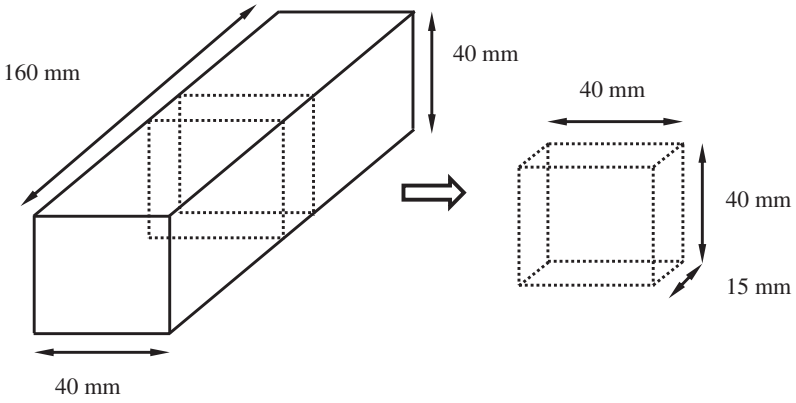

Fig. 7. Details of the sampling for the microscropy analysis.

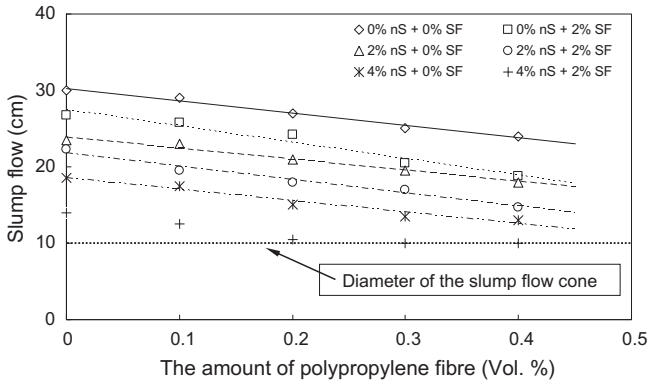

Fig. 8. Effect of nano-silica and hybrid fibres on the workability of the UHPFRC with waste bottom ash (WBA) (nS: Nano-silica, SF: Steel fibres).

fibres and concrete matrix and reduce the workability. Additionally, the effect of nano-silica on the flowability of concrete should be attributed to the increase of the viscosity of cement paste. Berra [52] explained that the significant water retention capacity of cement paste with nano-silica should be attributed to instantaneous interactions between nano-silica slurry and the liquid phase of cement pastes. One hypothesis is proposed that the presence of nano-silica decreases the amount of lubricating water available within the interparticle voids, which causes an increase of yield stress and plastic viscosity of concrete [53]. In the present day, due to the multiple effects from nano-silica and hybrid fibres on the workability of UHPFRC, the flowability of the sample simultaneously containing nano-silica (4%), steel fibres (2 vol.%) and polypropylene fibre (0.3 or 0.4 vol.%) can reduce to zero.

To summarize, in this study, after utilizing WBA to replace about 20% aggregates, the workability of the designed UHPFRC obviously decreases, compared to the one without WBA. Moreover, the addition of nano-silica, steel and polypropylene fibres can further reduce the flowability of the UHPFRC with WBA. Hence, it is important to properly adjust the water and superplasticizer amounts to obtain a flowable UHPFRC with WBA.

3.2. Porosity of the UHPFRC with WBA

Fig. 9 presents the effect of nano-silica and hybrid fibres on the porosity of the UHPFRC with WBA. It is obvious that the porosity of the designed UHPFRC is relatively high, with around 17 vol.%. From the prelliminary experiments, it was found that the porosity of the designed UHPFRC without WBA is about 10%, which means that about 7% of the porosity should be arrtibuted to the addition of WBA. Based on the literature [29–31], the metallic aluminium particles in WBA react in the alkaline environment in concrete and release hydrogen, which influences the microstructure development and produce cracks. Hence, in this study, just due to the existence of metallic aluminium (as shown in Table 2), the porosities of the designed UHPFRC are relatively high. Moreover, it can be noticed that the addition of steel fibres can significantly further increase the porosity of the UHPFRC, while the polypropylene fibres only slightly increase the porosity of the UHPFRC. These phenomena should be attributed to the fact that the steel fibre could change the structure of the granular skeleton, while flexible fibres fill the space between the large particles. Nevertheless, it is improtant to notice that the porosity of the UHPFRC slightly decreases with the addtion of nano-silica. For instance, in the samples without fibres, the addition of about 4% nano-silica can reduce the porosity of the UHPFRC from about 16.8% to 16.5%. This should be attributed to the nucleation and pozzolanic effect of nano-silica during the cement hydration. As commonly known, due to the nucleation effect, the formation of C–S–H-phase is no longer restricted on the cement grain surface alone, which cause that the hydration degree of cement is higher and more pores can be filled by the newly generated C–S–H [54]. Therefore, the new generated C–S–H gel can effectively fill the pores of the concrete and simutaneously decrease its porosity.

In a short summary, the inclusion of WBA causes that the porosity of the designed UHPFRC is relatively high. Additionally, the addition of steel and polypropylene fibres could both increase the porosity of the concrete. However, appropriate addition of nano-silica can slightly reduce the porosity of the concrete.

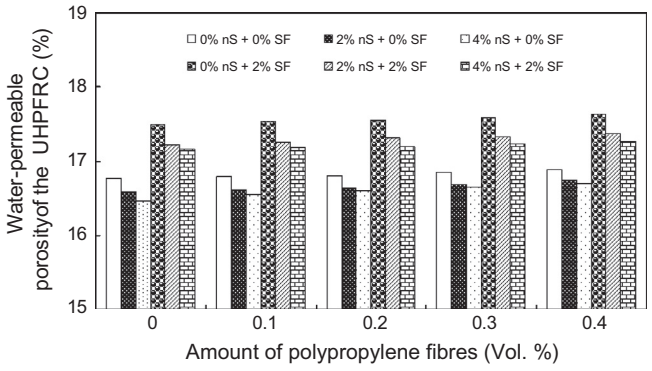

Fig. 9. Effect of nano-silica and hybrid fibres on the porosity of the UHPFRC with waste bottom ash (WBA) (nS: Nano-silica, SF: Steel fibres).

3.3. Flexural strength of UHPFRC with WBA

In this study, to better understand the effect of nano-silica and hybrid fibres on the flexural strength of the UHPFRC with WBA, the 3-point flexural test is executed, and the results are compared in different groups, which are "single factor effect", "dual factors effect" and "triple factors effect", as presented in the following part.

3.3.1. Single factor effect

The single factor effect of steel fibres on the flexural strength of UHPFRC with WBA is shown in Fig. 10. Similarly to the results shown in other studies, the addition of steel fibres (2 vol.%) does not only enhance the ultimate flexural strength, but also improves the energy absorption capacity of the designed UHPFRC. This should be attributed to the fact that the additional steel fibres can bridge cracks and retard their propagation, which could change the fracture mode of concrete from brittle fracture to plastic fracture and significantly increase the ultimate flexural strength of concrete [32,33]. However, compared to the results available in the literature [14–16], it can also be noticed that the ultimate flexural strength of the UHPFRC (shown in Fig. 11) is relatively smaller, which amounts to 11.6 MPa without steel fibre and 18.8 MPa with 2% steel fibre, respectively. This should be attributed to the negative influence of the additional WBA. The metallic aluminium particles in WBA react in the alkaline enviroment in concrete and release hydrogen, which may influence the microstructure development and produce cracks. Though the steel fibres can retard the propagation of the macro-cracks, the development of the micro-cracks may also significantly reduce the mechanical properties.

Fig. 11 presents the single effect of nano-silica on the flexural strength of UHPFRC with WBA. It is clear that the addition of nano-silica can improve the ultimate flexural strength of the designed UHPFRC with WBA. For instance, the ultimate flexural strength of the sample with 4% nano-silica is 14.3 MPa, which is obviously larger than the one without nano-silica (11.6 MPa). This should be attributed to the nucleation and pozzolanic effect of nano-silica, as already explained in Section 3.2. Hence, the interface between the matrix and aggregate could become much stronger, and the concrete strength could be simultaneously high.

The single effect of polypropylene fibres on the flexural strength of UHPFRC with WBA is illustrated in Fig. 12. Differently from the effect of steel fibre, the fracture mode of the samples with polypropylene fibres is still the brittle fracture, as for the reference sample. Moreover, the addition of polypropylene fibres can slightly increase the ultimate flexural strength and energy absorption capacity of the UHPFRC, which should be attributed to the fact that the polypropylene fibres have good ductility, fineness and dispersion, so they can restrain the plastic cracks [55]. Nevertheless, the elastic

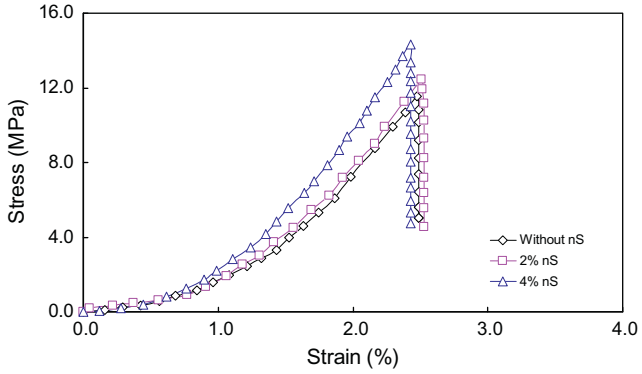

Fig. 11. Effect of the nano-silica (nS) on the flexural strength of UHPFRC with waste bottom ash (WBA).

modulus and stiffness of polypropylene fibres are much lower than that of steel fibre, which cause that the improvement of the ultimate flexural strength and energy absorption capacity are not obvious.

3.3.2. Dual factors effect

Fig. 13 shows the dual effect from steel fibres and nano-silica on the flexural strength of UHPFRC with WBA. It is important to notice that the ultimate flexural strength and energy absorption capacity of the sample with both steel fibres and nano-silica are much larger than that of the reference sample. Especially for the one with steel fibre (2 vol.%) and nano-silica (4%), the ultimate flexural strength is about 28 MPa. This should be attributed to the multiple effects of steel fibres and nano-silica. The nucleation effect of nano-silica in concrete can cause that the steel fibres are tightly caught by the matrix, which means more energy is needed to break the UHPFRC, and its energy absorption capacity is significantly enhanced.

The multiple effects of steel fibres and polypropylene fibres on the flexural strength of UHPFRC with WBA are presented in Fig. 14. Note that the addition of polypropylene fibres can further improve the ultimate flexural strength and the energy absorption capacity of the steel fibre reinforced samples. For instance, the ultimate flexural strength of the sample with steel fibres (2 vol.%) and polypropylene fibres (0.4 vol.%) of is about 25 MPa, which is clearly larger than the one with steel fibres only (about 19 MPa). As shown in [32–33], short fibres can bridge micro-cracks more efficiently, because they are very thin and their number in concrete is much larger than that of the long steel fibres, for the same fibre volume. Hence, when the micro-cracks are just generated in the concrete specimen, the short polypropylene fibres can effectively bridge

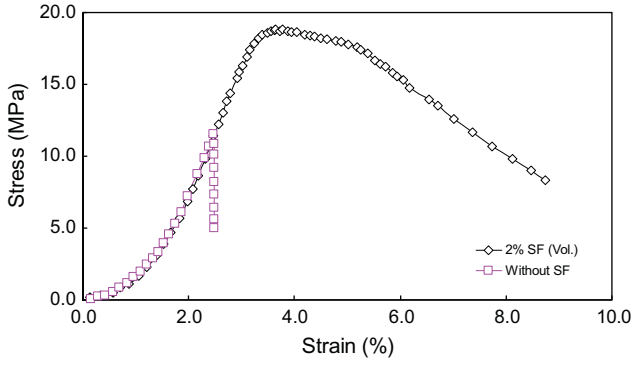

Fig. 10. Effect of the steel fibre (SF) on the flexural strength of UHPFRC with waste bottom ash (WBA).

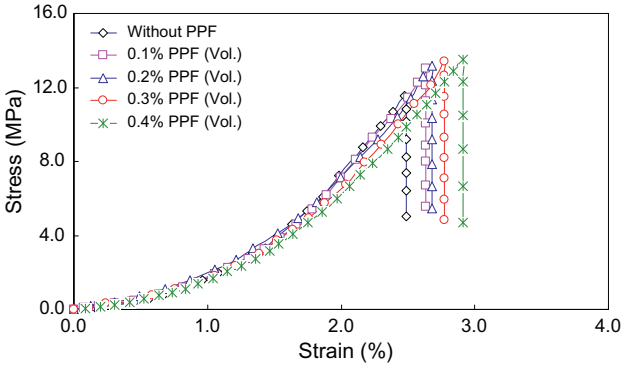

Fig. 12. Effect of the polypropylene fibres (PPF) on the flexural strength of UHPFRC with waste bottom ash (WBA).

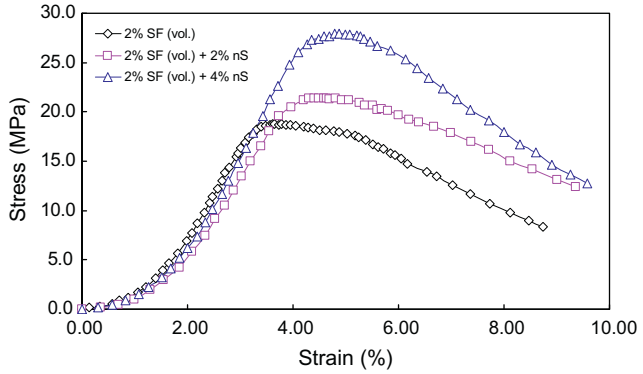

Fig. 13. Dual effects of the steel fibre (SF) and nano-silica (nS) on the flexural strength of UHPFRC with waste bottom ash (WBA).

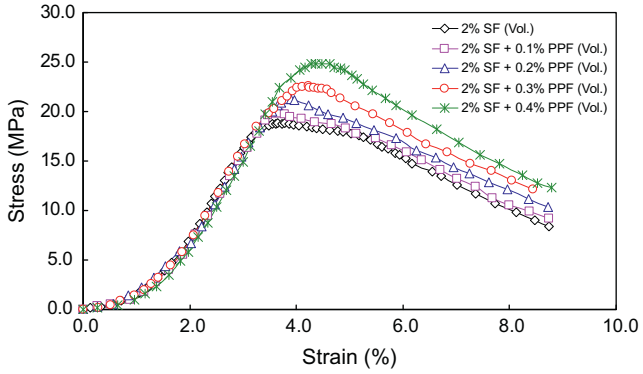

Fig. 14. Dual effects of the steel fibre (SF) and polypropylene fibres (PPF) on the flexural strength of UHPFRC with waste bottom ash (WBA).

the micro-cracks. As the micro-cracks grow and join into larger macro-cracks, the long steel fibres become more active in crack bridging. In this way, primarily the ductility can be improved, and partly also the flexural strength. Long fibres can therefore provide a stable post-peak response. Short fibres will then become less active, because they are being pulled out, as the crack width increases.

However, a simultaneous inclusion of nano-silica and polypropylene fibres in the UHPFRC with WBA cannot effectively enhance its flexural strength, which is illustrated in Fig. 15. The fracture mode of all the tested samples is the brittle fracture mode, and the enhancement of the ultimate flexural strength is also limited. For example, the ultimate flexural strength of the sample with nano-silica (4%) and polypropylene fibres (0.4 vol.%) is about 18 MPa, which is relatively low. This should be attributed to the fact that although the interface between the matrix and fibres is improved by the addition of nano-silica, the polypropylene fibres are still less effective in bridging the macro-cracks.

Consequently, it can be predicted that to obtain the UHPFRC with superior flexural strength, the steel fibres, polypropylene fibres and nano-silica should be simultaneously included in the concrete design.

3.3.3. Triple factors effect

The triple effect from nano-silica and hybrid fibres on the flexural strength of the designed UHPFRC is depicted in Fig. 16. Here, only four typical curves are selected and compared. It is important to notice that the ultimate flexural strength of the sample with nano-silica (4%), steel fibre (2 vol.%) and polypropylene fibres (0.4 vol.%) is around 32 MPa, which is comparable to that of normal

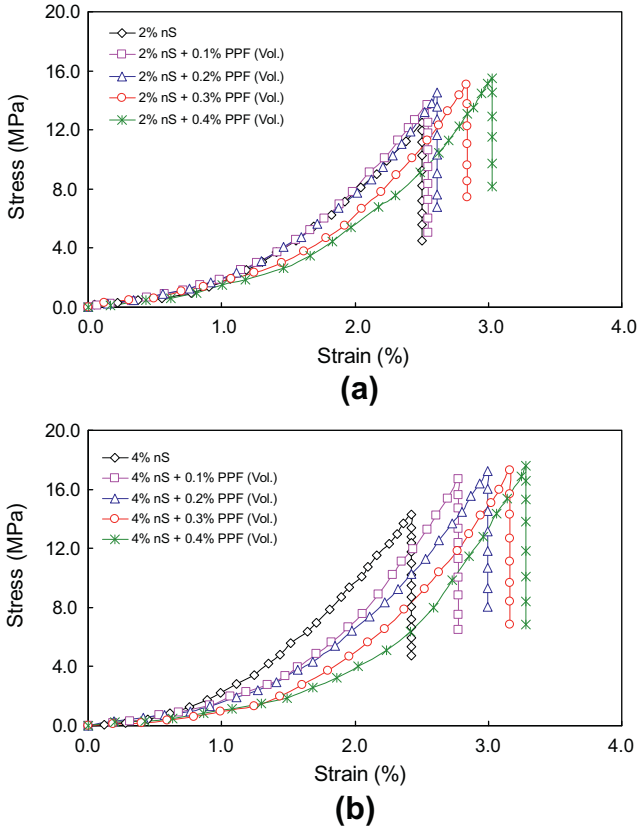

Fig. 15. Dual effects of the nano-silica (nS) and polypropylene fibres (PPF) on the flexural strength of UHPFRC with waste bottom ash (WBA).

UHPFRCs without any waste materials [14–16]. This should be attributed to the multiple effects of nano-silica and hybrid fibres. The polypropylene fibres bridge the micro-cracks and the steel fibres restrict the development of the macro-cracks. Moreover, the additional nano-silica can strengthen the interface between the fibres and matrix, so more energy can be absorbed by the samples.

3.4. Compressive strength of UHPFRC with WBA

The compressive strength of the designed UHPFRC with WBA is shown in Fig. 17. As can be seen, the additional steel fibre could significantly increase the compressive strength of the UHPFRC. For instance, the compressive strength of the samples without steel

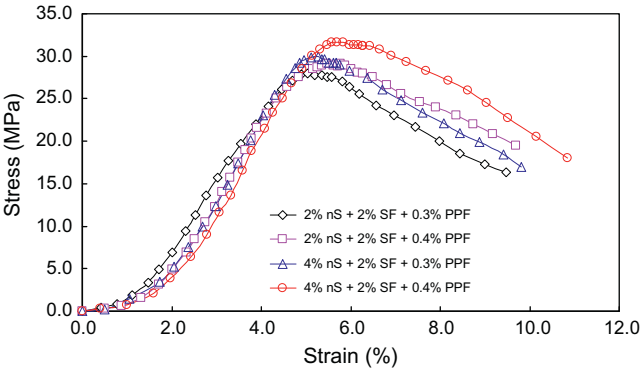

Fig. 16. Triple effects of the nano-silica (nS), steel fibres (SF) and polypropylene fibres (PPF) on the flexural strength of UHPFRC with waste bottom ash (WBA).

fibres fluctuates around 70 MPa, while the compressive strength of the steel fibre reinforced sample sharply increases to about 115 MPa. Furthermore, with an increase of the nano-silica amount, the compressive strength of the concrete slightly increases. Additionally, it can be observed that the effect of polypropylene fibres on the compressive strength is not significant. Nevertheless, it still can be noticed that the compressive strength of the designed UHPFRC is relatively lower than that of other UHPFRC [14–16]. This should be attributed to the following reasons: (1) the used WBA can generate hydrogen and affect the microstructure development of the concrete, which can increase the porosity and decrease the compressive strength of the concrete; (2) the quality of the used WBA is relatively poor, as it contains some impurities that have no contribution or negative contribution to the compressive strength development.

A summary of the effect of nano-silica, steel fibres and polypropylene fibres on the mechanical properties of the concrete is shown in Table 4. It is clear that with the inclusion of the WBA in concrete, the compressive strength sharply decreases, while the flexural strength is relatively comparable. However, a simultaneous inclusion of nano-silica, steel fibres and polypropylene fibres can significantly improve the mechanical properties of the concrete (especially the flexural strength). Hence, the UHPFRC with WBA can be produced and utilized in the place with high flexural strength requirements.

3.5. Hydration process of the UHPFRC with WBA

To clearly understand the effect of nano-silica on the properties of the UHPFRC with WBA, the isothermal calorimetry is utilized to analyze its hydration process, and the results of these analyses are shown in Fig. 18. It is apparent that with the addition of WBA, the height of the early rate peak is reduced, and the time required to reach the maximum rate is simultaneously extended. These imply that the hydration of cement is slightly retarded by the additional WBA, which is in line with the results presented in [56,57]. From Table 2 and Fig. 4, it can be noticed that are many impurities in the utilized WBA, which may affect the hydration of cement. Moreover, the addition of nano-silica can significantly accelerate the cement hydration, and with the increased amount of nano-silica, the cement hydration rate simultaneously rises. Eventually, in this study, the additional nano-silica could compensate the negative influence of WBA on the hydration of cement. This phenomenon should be attributed to the nucleation and pozzolanic effect from nano-silica. After mixing, the nanoparticles are uniformly dispersed in concrete. When the hydration begins, the hydration products diffuse and envelop nanoparticles as kernels, which can promote the cement hydration and makes the cement

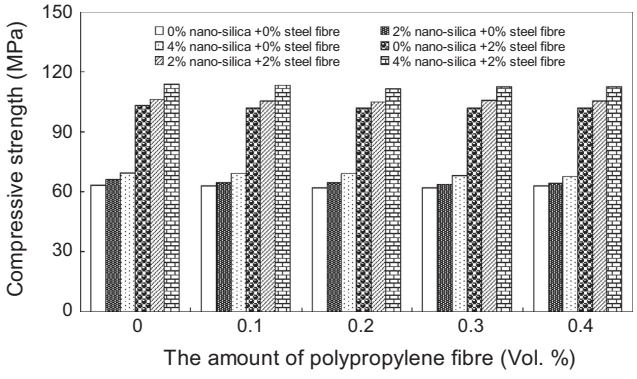

Fig. 17. Compressive strength of UHPFRC with waste bottom ash (WBA) after curing for 28 days.

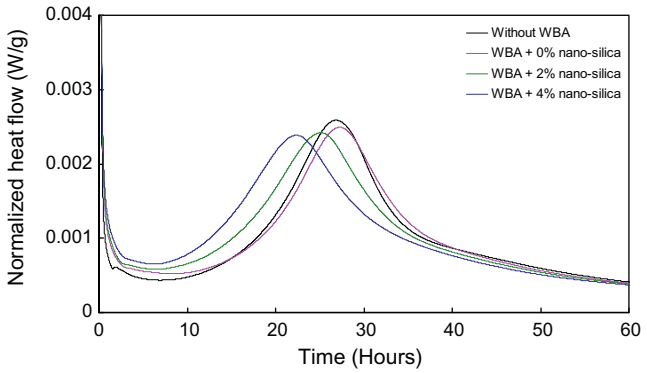

Fig. 18. Calorimetry test results of designed UHPFRC with different amount of nano-silica.

matrix more homogeneous and compact [58]. Therefore, in this study, with the increase of nano-silica amount, more reactive kernels will be generated during the hydration, so in turn the hydration rate of cement is accelerated.

The hydration process of cement can be classified into four principle stages [59]: (1) initial phases of dissolved substances; (2) induction period where the C–S–H and portlandite-nucleation begins; (3) the acceleration period begins about one hour after mixing the cement with water; (4) After about three hours the reaction gets controlled by the diffusion and the heat evolution rate starts to decrease. However, in this study, the induction and acceleration period of cement hydration are obviously longer than a normal cement. For instance, in the sample without WBA, the induction and acceleration period are about 10 h and 15 h, respectively (see Fig. 18). This should be attributed to the retardation influence of the superplasticizer. According to the investigation of Jansen [60], complex Ca^{2+} ions from pore solution by the superplasticizer should be the substance that can absorb the polymer on the nuclei or the anhydrous grain surfaces, which in turn might lead to the prevention of the growth of the nuclei or the dissolution of the anhydrous grains. Hence, in this study, due to the fact that high amount of superplasticizer is utilized to produce the UHPFRC, the cement hydration is significantly retarded.

3.6. Microscopy analysis of the UHPFRC with WBA

To clarify the effect of the hybrid fibres on the mechanical properties of the UHPFRC with WBA, the microscopy images of the different samples are compared, which is shown in Fig. 19.

As can be seen in Fig. 19a, the microstructure of the designed UHPFRC is dense and homogeneous, which should be attributed to the low water to cement ratio and the optimized particle packing. In this study, the design of the UHPFRC is based on the aim to achieve a densely compacted cementitious matrix, employing the modified Andreasen and Andersen particle packing model. Hence, this also demonstrates that it is possible to utilize particle packing model to design UHPFRC incorporating waste materials. However, from Fig. 19b, a relatively long and narrow macro-crack can be observed. The length of the crack is about 4.75 mm, which is more than two times the diameter of the maximum aggregate in concrete. The generation of the macro-cracks should be attributed to the chemical reaction of the metallic aluminium particles in WBA with the alkaline solution in concrete can generate hydrogen. Supposing that the generated hydrogen cannot timely escape from the concrete in fresh state, it will gradually produce a series of micro-cracks in the hardened concrete. With the increase and the interconnections of the micro-cracks, the visible macro-cracks could be created. Moreover, due to the fact that the distribution

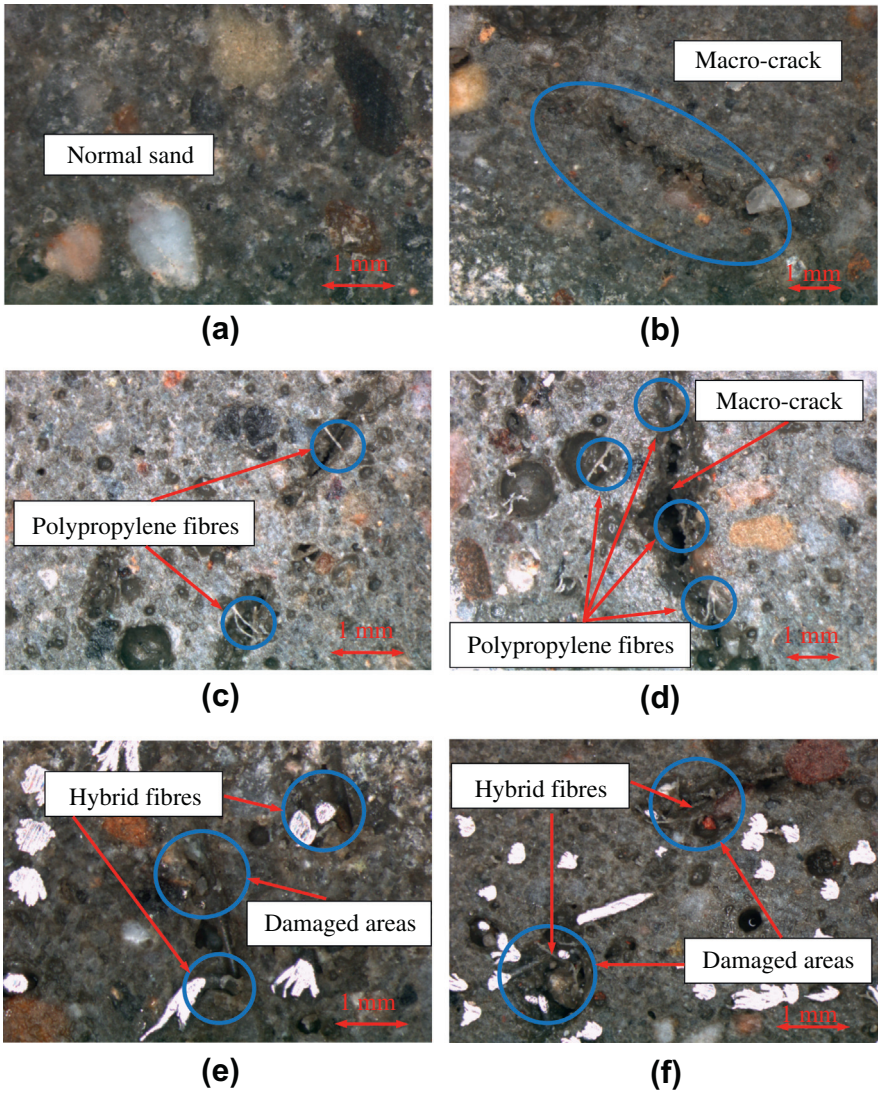

Fig. 19. Microscopy images of the designed UHPFRC with waste bottom ash (WBA).

of the metallic aluminium particles is heterogeneous, the distribution of the visible macro-cracks is also inhomogeneous. Hence, during the mechanical tests, the stresses may concentrate around the cracks and eventually reduce the mechanical properties of the UHPFRC.

Fig. 19c and d illustrate the microscopy images of the samples with only polypropylene fibres. As shown in Fig. 19b, some visible macro-cracks can still be found, and the length of the indicated crack is about 4.4 mm. Moreover, around the cracks, many polypropylene fibres can be observed, some of which even bridge the cracks. From the literature [61–63], it can be stated that the polypropylene fibres can contribute to the concrete performance subjected to crack opening and slippage. Nevertheless, here, the addition of polypropylene fibres is less efficient in restricting the generation of the macro-cracks (compared to the steel fibres), which causes that the mechanical properties of the sample with only polypropylene fibres are relatively poor (Fig. 12). This may be attributed to the following reasons: (1) the macro-cracks are created before the hardening of concrete, which means the interface between the polypropylene fibres and the matrix is still quite weak and the fibres could not effectively bridge the cracks; (2) the size of the used polypropylene fibres in some cases is even smaller than the length of the macro-cracks, which causes that the fibres are useless in restricting the development of this type macro-cracks.

The microscopy images of the sample simultaneously containing nano-silica (4%), steel fibres (2 vol.%) and polypropylene fibres (0.4 vol.%) are shown in Fig. 19e and f. It is important to notice that although the mechanical properties of this sample are superior, a damaged microstructure can still be observed. Nevertheless, the damage area is much smaller than that shown in Fig. 19b–d. Furthermore, close to the damage area, many hybrid fibres can be found, and the interface between these fibres and concrete matrix is still compact and tight. As the results shown in [33], in hybrid-fibre concrete, the short fibres can "help" the long fibres to generate high tensile stresses. Therefore, the combining of different types of fibres in the same concrete results in better mechanical behaviour compared to the concrete with only one single type of fibre. In this study, due to the addition of hybrid fibres into the UHPFRC, the short polypropylene fibres can restrict the development of the micro-cracks and the long steel fibres could hinder the generation of the macro-cracks. Hence, the damage caused by the generated hydrogen can be minimized, and the mechanical properties of the designed UHPFRC are improved.

Consequently, based on the microscopy analysis and calorimetry test results, the multiple effect of nano-silica and hybrid fibres on the mechanical properties should be summarized as following: (1) the addition of hybrid fibres can effectively minimize the damage originating from the generated hydrogen and reduce the stress

concentration under the external loading; (2) the additional nano-silica could promote the hydration of cement and improve the bond between matrix, aggregate and fibres.

4. Conclusions

This paper presents the multiple effects of nano-silica and hybrid fibres on the properties of an Ultra-High Performance Fibre Reinforced Concrete (UHPFRC) incorporating waste bottom ash (WBA). The design of the concrete mixtures was based on the aim to achieve a densely compacted cementitious matrix, employing the modified Andreasen and Andersen particle packing model. From the results addressed in this paper the following conclusions are drawn:

- By employing the Andreasen and Andersen particle packing model, it is possible to utilize waste bottom ash to produce UHPFRC with a relatively low binder amount (about 650 kg/m^3). The obtained maximum compressive and flexural strengths of the designed UHPFRC are about 115 and 32 MPa, respectively.
- When using WBA to replace about 20% of conventional aggregates, the workability of the designed UHPFRC decreases. Moreover, the addition of nano-silica, steel fibres and polypropylene fibres can further reduce the flowability of the UHPFRC with WBA. Hence, it is important to properly adjust the water and superplasticizer amounts to obtain a flowable UHPFRC with WBA.
- Due to the application of WBA, the water-permeable porosity of the designed UHPFRC is relatively high (about 17%). Moreover, the addition of steel and polypropylene fibres could both increase the porosity of the concrete. Nevertheless, an appropriate addition of nano-silica (around 4% by the mass of the binder) can slightly reduce the porosity of the concrete.
- The addition of WBA reduces the compressive strength of the designed concrete. However, due to the coarse surface of WBA and the threadlike stuff on its surface, the flexural strength of the designed concrete can be slightly enhanced. After the nano-silica and hybrid fibres are added into the concrete, its mechanical properties (especially the flexural strength) can be significantly improved. Hence, the UHPFRC with WBA can be produced and utilized in concretes with high flexural strength requirements.
- The addition of WBA can slightly retard the cement hydration. However, the small dosage of the additional nano-silica could compensate this retarding influence of WBA on the hydration rate of cement, which is attributed the nucleation effect of nano-silica.
- The microstructure development of concrete is influenced and some macro-cracks could be generated due to the addition of WBA. However, the simultaneous addition of nano-silica and hybrid fibres into UHPFRC can effectively restrict and minimize the cracks, which causes that the mechanical properties of the designed UHPFRC with WBA could be significantly improved.

Acknowledgements

The authors wish to express their gratitude to Bekaert for supplying the steel fibres and to the following sponsors of the Building Materials research group at TU Eindhoven: Graniet-Import Benelux, Kijlstra Betonmortel, Struyk Verwo, Attero, Enci, Provincie Overijssel, Rijkswaterstaat Zee en Delta – District Noord, Van Gansewinkel Minerals, BTE, V.d. Bosch Beton, Selor, Twee "R" Recycling, GMB, Schenk Concrete Consultancy, Geochem Research, Icopal, BN International, Eltomation, Knauf Gips, Hess ACC Systems, Kronos, Joma, CRH Europe Sustainable Concrete Centre, Cement&BetonCentrum and Heros (in chronological order of joining).

References

[1] Richard P, Cheyrezy M. Composition of reactive powder concretes. Cem Concr Res 1995;25(7):1501–11.
[2] Yang SL, Millard SG, Soutsos MN, Barnett SJ, Le TT. Influence of aggregate and curing regime on the mechanical properties of ultra-high performance fibre reinforced concrete (UHPFRC). Constr Build Mater 2009;23:2291–8.
[3] Habert G, Denarié E, Šajna A, Rossi P. Lowering the global warming impact of bridge rehabilitations by using Ultra High Performance Fibre Reinforced Concretes. Cem Concr Comp 2013;38:1–11.
[4] UNSTATS. Greenhouse gas emissions by sector (absolute values). United Nation Statistical Division: Springer; 2010.
[5] Friedlingstein P, Houghton RA, Marland G, Hackler J, Boden TA, Conway TJ, et al. Uptake on CO_2 emissions. Nat Geosci 2010;3:811–2.
[6] Capros P, Kouvaritakis N, Mantzos L. Economic evaluation of sectorial emission reduction objectives for climate change top–down analysis of greenhouse gas emission possibilities in the EU. Contribution to a study for DG environment. European commission; 2001.
[7] Denarié E, Brühwiler E. Strain hardening ultra-high performance fibre reinforced concrete: deformability versus strength optimization. Int J Rest Build Monuments 2011;17(6):397–410 [Aedificatio].
[8] Brühwiler E, Denarié E. Rehabilitation of concrete structures using ultra-high performance fibre reinforced concrete. In: Proceedings, UHPC-2008: the second international symposium on ultra-high performance concrete, March 05–07, 2008, Kassel, Germany.
[9] Toledo Filho RD, Koenders EAB, Formagini S, Fairbairn EMR. Performance assessment of ultra-high performance fibre reinforced cementitious composites in view of sustainability. Mater Des 2012;36:880–8.
[10] De Larrard F, Sedran T. Optimization of ultra-high-performance concrete by the use of a packing model. Cem Concr Res 1994;24:997–1009.
[11] De Larrard F, Sedran T. Mixture-proportioning of high-performance concrete. Cem Concr Res 2002;32:1699–704.
[12] Stark U, Mueller A. Optimization of packing density of aggregates. In: Proceedings of the second international symposium on ultra-high performance concrete. Kassel, Germany, March 05–07; 2008.
[13] Yu R, Spiesz P, Brouwers HJH. Mix design and properties assessment of Ultra-High Performance Fibre Reinforced Concrete (UHPFRC). Cem Concr Res 2014;56:29–39.
[14] El-Dieb AS. Mechanical, durability and microstructural characteristics of ultra-high-strength self-compacting concrete incorporating steel fibres. Mater Des 2009;30:4286–92.
[15] Tayeh BA, Abu Bakar BH, Megat Johari MA, Voo YL. Mechanical and permeability properties of the interface between normal concrete substrate and ultra-high performance fibre concrete overlay. Constr Build Mater 2012;36:538–48.
[16] Hassan AMT, Jones SW, Mahmud GH. Experimental test methods to determine the uniaxial tensile and compressive behaviour of ultra-high performance fibre reinforced concrete (UHPFRC). Constr Build Mater 2012;37:874–82.
[17] Tuan NV, Ye G, Breugel K, Copuroglu O. Hydration and microstructure of ultra-high performance concrete incorporating rice husk ash. Cem Concr Res 2011;41:1104–11.
[18] Tuan NV, Ye G, Breugel K, Fraaij ALA, Dai BD. The study of using rice husk ash to produce ultra-high performance concrete. Constr Build Mater 2011;25:2030–5.
[19] Aldahdooh MAA, Muhamad Bunnori N, Megat Johari MA. Development of green ultra-high performance fibre reinforced concrete containing ultrafine palm oil fuel ash. Constr Build Mater 2013;48:379–89.
[20] Vejmelková E, Keppert M, Rovnaníková P, Ondráček M, Keršner Z, Černy R. Properties of high performance concrete containing fine-ground ceramics as supplementary cementitious material. Constr Build Mater 2012;34:55–61.
[21] Chimenos JM, Segarra M, Fernández MA, Espiell F. Characterization of the bottom ash in a municipal solid waste incinerator. J Hazard Mater 1999;A64:211–22.
[22] CEC, Council Directive 1999/31/ EC of 26 April 1999 on the landfill ofwaste, Off. J. Eur. Communities, 16/7/1999, L182/1-19.
[23] Izquierdo M, Vazquez E, Querol X, Barra M, López A, Plana F. Use of bottom ash from municipal solid waste incineration as a road material. In: International ash utilization symposium, 4th, Lexington, KY, United States; 2001. p.31–8.
[24] Forteza R, Far M, Seguí C, Cerdá V. Characterization of bottom ash in municipal solid waste incinerators for its use in road base. Waste Manage 2004;24:899–909.
[25] Ministerial Order PG-3/2004, Pliego de prescripciones técnicas generales para obras de carreteras y puentes, Ministry of Development, Order FOM/891/2004.
[26] Kim HK, Jeon JH, Lee HK. Flow, water absorption, and mechanical characteristics of normal and high-strength mortar incorporating fine bottom ash aggregates. Constr Build Mater 2012;26:249–56.
[27] Lee HK, Kim HK, Hwang EA. Utilization of power plant bottom ash as aggregates in fibre-reinforced cellular concrete. Waste Manage 2010;30:274–84.

[28] Kim HK, Lee HK. Use of power plant bottom ash as fine and coarse aggregates in high-strength concrete. Constr Build Mater 2011;25:1115–22.
[29] Pera J, Coutaz L, Ambroise J, Chababbet M. Use of incinerator bottom ash in concrete. Cem Concr Res 1997;27(1):1–5.
[30] Müller U, Rübner K. The microstructure of concrete made with municipal waste incinerator bottom ash as an aggregate component. Cem Concr Res 2006;36:1434–43.
[31] Qiao XC, Tyrer M, Poon CS, Cheeseman CR. Characterization of alkali-activated thermally treated incinerator bottom ash. Waste Manage 2008;28:1955–62.
[32] Grünewald S. Performance-based design of self-compacting fibre reinforced concrete. Delft, The Netherlands: Delft University of Technology; 2004.
[33] Markovic I. High-performance hybrid-fibre concrete development and utilization. Delft, The Netherlands: Delft University of Technology; 2006.
[34] Pan JR, Huang C, Kuo JJ, Lin SH. Recycling MSWI bottom and fly ash as raw materials for Portland cement. Waste Manage 2008;28:1113–8.
[35] Nazari A, Riahi S. The effects of SiO_2 nanoparticles on physical and mechanical properties of high strength compacting concrete. Compos B Eng 2011;42:570–8.
[36] Li H, Xiao H, Yuan J, Ou J. Microstructure of cement mortar with nano-particles. Compos B Eng 2004;35:185–9.
[37] Fuller WB, Thompson SE. The laws of proportioning concrete. Trans Am Soc Civil Eng 1907;33:222–98.
[38] Andreasen AHM, Andersen J. Über die Beziehungen zwischen Kornabstufungen und Zwischenraum in Produkten aus losen Körnern (mit einigen Experimenten). Kolloid-Zeitschrift 1930;50:217–28 (In German).
[39] Funk JE, Dinger DR. Predictive process control of crowded particulate suspensions, applied to ceramic manufacturing. Boston, the United States: Kluwer Academic Publishers; 1994.
[40] Brouwers HJH, Radix HJ. Self compacting concrete: theoretical and experimental study. Cem Concr Res 2005;35:2116–36.
[41] Hüsken G. A multifunctional design approach for sustainable concrete with application to concrete mass products. PhD thesis. Eindhoven University of Technology, Eindhoven, the Netherlands; 2010.
[42] Hunger M. An integral design concept for ecological self-compacting concrete. PhD thesis. Eindhoven University of Technology, Eindhoven, the Netherlands; 2010.
[43] Yu QL, Spiesz P, Brouwers HJH. Development of cement-based lightweight composites – Part 1: Mix design methodology and hardened properties. Cem Concr Comp 2013;44:17–29.
[44] Spiesz P, Yu QL, Brouwers HJH. Development of cement-based lightweight composites – Part 2: Durability related properties. Cem Concr Comp 2013;44:30–40.
[45] Hüsken G, Brouwers HJH. A new mix design concept for each-moist concrete: a theoretical and experimental study. Cem Concr Res 2008;38:1249–59.
[46] Brouwers HJH. Particle-size distribution and packing fraction of geometric random packings. Phys. Rev. E 2006;74:031309-1–031309-14.
[47] BS-EN-1015-3, Methods of test for mortar for masonry – Part 3: Determination of consistence of fresh mortar (by flow table). In: British Standards Institution-BSI and CEN European Committee for Standardization; 2007.
[48] Safiuddin Md, Hearn N. Comparison of ASTM saturation techniques for measuring the permeable porosity of concrete. Cem Concr Res 2005;35:1008–13.
[49] NT Build 492. Concrete, mortar and cement-based repair materials: Chloride migration coefficient from non-steady-state migration experiments. Nordtest method, Finland; 1999.
[50] ASTM C1202. Standard Test Method for Electrical Indication of Concrete's Ability to Resist Chloride Ion Penetration. In: Annual Book of ASTM Standards, vol. 04.02. American Society for Testing and Materials, Philadelphia, July, 2005.
[51] BS-EN-196-1. Methods of testing cement – Part 1: determination of strength. British Standards Institution-BSI and CEN European Committee for Standardization; 2005.
[52] Berra M, Carassiti F, Mangialardi T, Paolini AE, Sebastiani M. Effects of nanosilica addition on workability and compressive strength of Portland cement pastes. Constr Build Mater 2012;35:666–75.
[53] Senff L, Labrincha JA, Ferreira VM, Hotza D, Repette WL. Effect of nano-silica on rheology and fresh properties of cement pastes and mortars. Constr Build Mater 2009;23(7):2487–91.
[54] Thomas JJ, Jennings HM, Chen JJ. Influence of nucleation seeding on the hydration mechanisms of tricalcium silicate and cement. J Phys Chem C 2009;113(11):4327–34.
[55] Saeid K, Hazizan MA, Morteza J, Jalal R. The effects of polypropylene fibres on the properties of reinforced concrete structures. Constr Build Mater 2012;27:73–7.
[56] Li XG, Lv Y, Ma BG, Chen QB, Yin XB, Jian SW. Utilization of municipal solid waste incineration bottom ash in blended cement. J Clean Prod 2012;32:96–100.
[57] Giampaolo C, Mastro SL, Polettini A, Pomi R, Sirini P. Acid neutralisation capacity and hydration behaviour of incineration bottom ash–Portland cement mixtures. Cem Concr Res 2002;32(5):769–75.
[58] Jalal M, Mansouri E, Sharifipour M, Pouladkhan AR. Mechanical, rheological, durability and microstructural properties of high performance self-compacting concrete containing SiO_2 micro and nanoparticles. Mater Des 2012;34:389–400.
[59] Land G, Stephan D. The influence of nano-silica on the hydration of ordinary Portland cement. J Mater Sci 2011;47(2):1011–7.
[60] Jansen D, Neubauer J, Goetz-Neunhoeffer F, Haerzschel R, Hergeth WD. Change in reaction kinetics of a Portland cement caused by a superplasticizer – calculation of heat flow curves from XRD data. Cem Concr Res 2012;42(2):327–32.
[61] Ramezanianpour AA, Esmaeili M, Ghahari SA, Najafi MH. Laboratory study on the effect of polypropylene fibre on durability, and physical and mechanical characteristic of concrete for application in sleepers. Constr Build Mater 2013;44:413–8.
[62] Noumowe A. Mechanical properties and microstructure of high strength concrete containing polypropylene fibres exposed to temperatures up to 200 °C. Cem Concr Res 2005;35:2192–8.
[63] Song PS, Hwang S, Sheu BC. Strength properties of nylon- and polypropylene–fibre-reinforced concretes. Cem Concr Res 2005;35:1546–50.